RSC Advances

REVIEW

View Article Online
View Journal | View Issue

Cite this: *RSC Adv.*, 2024, **14**, 3936

Recent advances in single-atom alloys: preparation methods and applications in heterogeneous catalysis

Shuang Zhang, Ruiying Wang, Xi Zhang * and Hua Zhao

Received 16th October 2023
Accepted 5th December 2023

DOI: 10.1039/d3ra07029h

rsc.li/rsc-advances

Single-atom alloys (SAAs) are a different type of alloy where a guest metal, usually a noble metal (*e.g.*, Pt, Pd, and Ru), is atomically dispersed on a relatively more inert (*e.g.*, Ag and Cu) host metal. As a type of atomic-scale catalyst, single-atom alloy catalysts have broad application prospects in the field of heterogeneous catalysis for hydrogenation, dehydrogenation, oxidation, and other reactions. Numerous experimental and characterization results and theoretical calculations have confirmed that the resultant electronic structure caused by charge transfer between the host metal and guest metal and the special geometric structure of the guest metal are responsible for the high selectivity and catalytic activity of SAA catalysts. In this review, the common methods for the preparation of single-atom alloys in recent years are introduced, including initial wet impregnation, physical vapor deposition, and laser ablation in liquid technique. Afterwards, the applications of single-atom alloy catalysts in selective hydrogenation, dehydrogenation, oxidation reactions, and hydrogenolysis reactions are emphatically reviewed. Finally, several challenges for the future development of SAA catalysts are proposed.

1 Introduction

In traditional bimetallic catalytic systems, heterogeneous metals mainly exist in the forms of alloys, core–shell structures, and heterostructures. Generally, the corresponding synergistic interactions between two metals significantly affect the catalytic selectivity and activity.[1–3] Alloying provides an efficient way to tailor the electronic and geometry structure, and thus tune the catalytic performance.[4] Zhang and many other researchers proposed and developed metal oxide-supported single-atom catalysts, which not only maximize the exposed catalytic active sites (significantly improving the catalytic activity) but also had unique geometrical and electronic structure characteristics (enhancing the selectivity of catalytic reactions).[5–11] Further, in 2012, Sykes doped single-atom Pd on the Cu (111) surface, and denoted this type of alloy material as a single-atom alloy (SAA).[12] They reported that the SAA has two key typical characteristics: (1) active metal atoms (especially noble metal, called guest metal) dispersed on the surface of a second metal (host metal) at the single-atom limit with a low concentration and (2) guest single atoms are thermodynamically more stable when surrounded by the host metal atom due to the formation of a metal–metal bond, which exists in the monodisperse state rather than larger ensembles, such as dimers and trimers.[13–18] This new type of material has been developed based on the combination of surface science, scanning probe microscopy on the surface of single crystals and the composition and evaluation of nano-alloy particles.[19–23]

SAAs are bimetallic alloy materials with a specific structure, where more active metal atoms are dispersed across the surface of a transition metal with a low concentration and anchored in the isolated state. Many studies have shown that compared with traditional bimetal alloy catalysts, the guest metal has the features of unique unsaturated coordination, special interaction between the host metal, the quantum size effect, *etc.*, which are different from traditional alloys.[24,25] Density functional theory (DFT) calculations confirmed that SAAs exhibit mean-field behavior with the absence of obvious energetic and spatial overlap between the host and guest atoms in SAAs, such as AgNi, AgPd, AgMn, AgCr, and AgCu. The valence electron structure of the guest metal in SAAs maintains good symmetry and is hardly disturbed by the host element.[26] Furthermore, no host–host metal bonding exists due to the isolated state of the host metals. The absence of host–host metal bonds results in the formation of a free-atom-like electronic structure on the gest element. Thus, the adsorption abilities of the host metal are altered when bonding with adsorbents compared with traditional nanoparticles.[27,28] Specifically, compared with the host metal element, SAAs have readily accessible active sites and free-atom-like electronic state, which are similar to homogeneous catalysts, providing a bridge between these two different fields.[29,30]

SAAs, as a new type of catalyst, exhibit special physicochemical and structural properties, as follows: (i) uniform active sites without influence from various interference site factors,

College of Chemistry and Materials Engineering, Beijing Technology and Business University, Beijing 100048, China

such as different vertices, steps and interfaces in nanoparticles, contributing to high selectivity; (ii) highly dispersed active site distribution, endowing them with higher intrinsic activity; (iii) more stable unique electronic and geometric coordination environment than the corresponding nanocatalysts; (iv) large bimetallic interface site, making SAAs model catalysts to study bimetallic co-catalysis sites, which is beneficial to reveal the mechanism of the catalytic reaction deeply; and (v) maximum utilization of predominant metal atom, greatly reducing the preparation cost, especially for noble metals.[31–35] The well-defined nature of the active sites of SAAs, which is different from their constituent metals, endows SAAs with unique catalytic activity and selectivity in many catalytic reaction fields, such as selective hydrogenation, dehydrogenation, oxidation and hydrogenolysis. Therefore, SAA catalysts have become one of the main classes of heterogeneous catalysts.[36–38]

2 Methods for the preparation of SAA catalysts

The method for the preparation of catalysts has a significant influence on their nanostructure. The design and synthesis of SAA catalysts based on the interaction between the guest and host metal are the premise of studying the structure–property relationship of SAAs. Gong *et al.* found that the exposed isolated Pt atoms in the Cu (111) surface are thermodynamically more stable compared with that in the Cu (100) surface and on the low-coordinated step edge and corner sites.[39] However, due to the differences in the physical and chemical properties of the two metal components, they tend to form their own single metal phase. Hence, for SAAs with the size limitation of alloy nanomaterials, it is necessary to avoid the agglomeration of the guest metal atoms, presenting great challenges in the synthesis conditions and methods for the preparation of SAAs. In recent years, with the continuous optimization of traditional catalyst synthesis methods, remarkable achievements related to the preparation of SAAs have also been made.[40] At present, the developed controllable synthesis strategies of SAA catalysts include initial wet impregnation, physical vapor deposition, step-wise reduction and pulsed laser liquid phase ablation.

2.1 Initial wet co-impregnation

Initial wet co-impregnation is one of the most common methods for preparing supported catalysts with the advantages of simple operation and low production cost. Similar to the general method for the preparation of bimetallic catalysts, the specific steps are as follows: (i) impregnation of precursor solution with two types of active metals on the support; (ii) adsorption process until adsorption equilibrium is reached; and (iii) separating, washing, drying and activation processing (*e.g.*, calcination and reduction).

Gong's group dispersed γ-Al_2O_3 in a $H_2PtCl_6 \cdot 6H_2O$ and $Cu(NO_3)_2 \cdot 3H_2O$ mixed precursor solution, followed by leaving it in the atmosphere statically overnight.[39] After drying in flowing air (80 °C, 12 h), the resulting precipitate was finally calcined (600 °C, 2 h). The lattice spacing of 0.21 nm was detected for the obtained sample, corresponding with that of Cu(111). No corresponding lattice spacing of the Pt crystal was observed, but isolated Pt atoms appeared and were continuously diluted with Cu(111), as confirmed by AS-HAADF-STEM. Also, *in situ* DRIFTS showed that the CO molecules were linearly adsorbed on individually dispersed Pt atoms. Thus, the combination of the characterization results of AC-HAADF-STEM and DRIFTS confirmed the successful preparation of the 0.1Pt10Cu SAA (Fig. 1). Keeping the Cu content constant at 10 wt% content, the Pt content could be varied from 0.025% to 0.1% without a change in the structure of the PtCu SAA.

Zhang *et al.* fabricated Ag-alloyed Pd SAA samples *via* the incipient wetness co-impregnation method using only ppm levels of Pd.[41] Notable, the Pd K-edge XANES white line of the above-mentioned AgPd SAA had a lower intensity and shifted to a lower energy compared with that of Pt foil, suggesting that charge transfer occurred from Ag to Pd. Also, they synthesized Cu-alloyed Pd single-atom catalysts using the incipient wetness

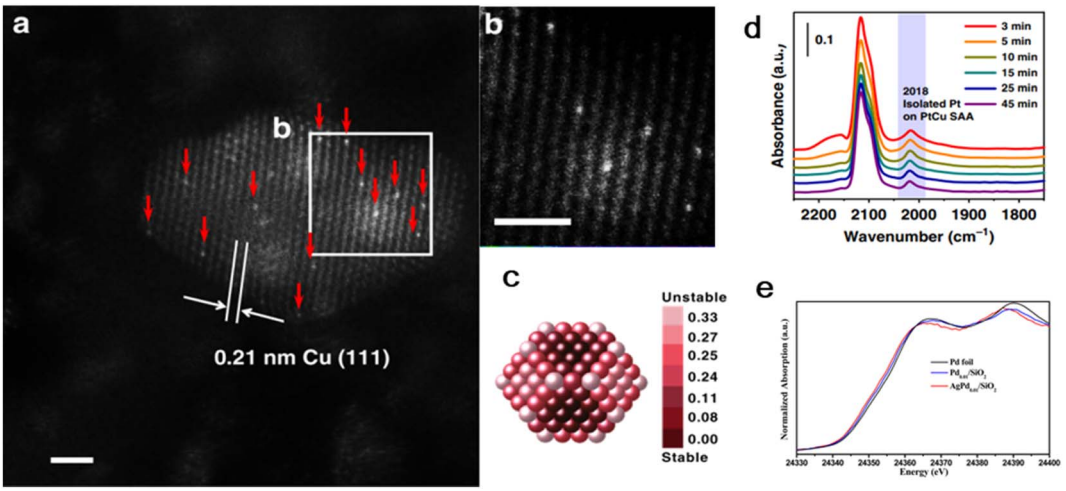

Fig. 1 (a) and (b) HAADF-STEM images of 0.1 Pt10Cu/Al_2O_3 catalyst. (c) Relative stability of Pt single atoms on Cu (~2.1 nm) nanoparticle. (d) *In situ* CO-DRIFTS and (e) normalized Pd K-edge XANES spectra of $AgPd_{0.01}/SiO_2$.[39]

co-impregnation method.[42] They found that Pd atoms can be fully isolated by Cu when the latter was more than 40 in the Cu/Pd atomic ratio. In the case of the PdCu SAA samples, the distances between atoms in the first shell of Pd were obviously shorter than that of Pd foil due to the formation of Pd–Cu coordination, and further increasing the Cu/Pd atomic ratio induced shorter distances in Pd–Cu (2.55 for $Cu_{40}Pd$ *vs.* 2.58 for $Cu_{160}Pd$). In addition, only Pd–Cu coordination was observed in the PdCu SAA catalysts and the coordination number of Pd–Cu increased with an increase in the Cu/Pd atomic ratio, while both Pd–Cu and Pd–Pd coordination existed in the $Cu_{12}Pd$ catalyst.

Therefore, both geometric and electronic synergistic effects between the Pd and Ag atoms were proven and high-temperature prereduction was shown to contribute to the optimal Pd/Ag surface composition with isolated electron-rich Pd atoms.

2.2 Step-wise reduction

When SAAs are prepared *via* the stepwise reduction method, the host metal NPs need to be synthesized *via* the reduction method first, followed by the generation of guest metal atoms on the host metal surface at the single-atom limit *via* further reduction. According to the different reduction methods of the loaded guest metal, it is mainly divided into galvanic replacement method, successive reduction method and electrochemical deposition method.[43,44]

2.2.1 Galvanic replacement method. The galvanic replacement (GR) method offers a simple route for the preparation of SAA catalysts.[45] Based on the different reduction potentials of the guest and host metal precursors, the GR reaction may or may not be thermodynamically favorable. Given that the host metal possesses lower reduction potentials than that of the guest metal, the replacement of the host metal by guest metal can occur spontaneously.[46,47] Especially, a small amount of guest metal favors the formation of a host-guest metal bond only, while avoiding the generation of guest–guest metal bonds. Generally, high-intensity ultrasound using a sonicator can facilitate the GR reaction rate, improve the metal dispersion and avoid the formation of dimers or trimers of guest metal.[48] For example, the reduction potential of Pt ($PtCl_6^{2-}$/Pt, E_0 = +1.44 V) is higher than that of Cu (Cu^{2+}/Cu, E_0 = +0.34 V), and thus the Cu host metal can be reduced by Pt^{4+} *via* the thermodynamically favorable redox reaction, as follows:

$$2Cu\ (s) + PtCl_6^{2-}\ (aq) = 2Cu^{2+}\ (aq) + Pt\ (s) + 6Cl^-\ (\Delta E^0 = +0.575\ V) \quad (1)$$

In addition, the corresponding large potential difference (up to 0.76 V) makes the reaction feasible and guarantees that the replacement reaction occurs rapidly even at T = 0 °C. The nanoscale Kirkendall-effect-induced hollowing process between $PtCl_6^{2-}$ ions and Cu particles/clusters during the GR reaction can account for the possible formation mechanism, enabling the deposition of Pt on the Cu surface to form the Pt–Cu alloy.[48,49] According to the above-mentioned equation, the consumption of two Cu atoms can deposit one Pt atom, meanwhile leaving redundant lattice vacancies on the surface of the Cu particles. Due to the non-compensation of less Pt atoms for the vacancies left by the reduction of Cu atoms, a higher surface free energy is generated.

The formation of SAAs *via* the GR reaction was reported by Mohl and co-workers.[50] They successfully applied the GR method to construct CuPd and CuPt SAAs with different compositions by controlling the amount of Pd and Pt salts added. Cu nanostructures are the suitable sacrificial templates due to their advantages of low cost and easy production purification. Generally, in the case of reduced Cu nanowires or nanoparticles, their color turns to dark gray after the introduction of precious metal salts, suggesting the replacement of Cu by Pt or Pd during the GR reaction and formation of CuPt and/or CuPd SAAs.[51] In terms of reaction media, besides dilute water, dimethyl sulfoxide has been used as a polar aprotic solvent to prevent some host particles from agglomerating in distilled water.[50] However, Mohl *et al.* found that Pt and Pd ions tended to aggregated to form the corresponding nanoparticles in ethanol solvent.

Flytzani-Stephanopoulos *et al.* prepared a PdCu SAA with a Pd/Cu atomic ratio of 0.18% supported on Al_2O_3 by the GR reaction.[46] Firstly, Cu nanoparticles were synthesized by $NaBH_4$ reduction in the presence of PVA, followed by adsorption on Al_2O_3 to obtain the supported Cu catalyst. After reduction in a hydrogen atmosphere at 250 °C at a rate of 5 °C min^{-1}, Cu/Al_2O_3 was transferred to an aqueous solution with a immersed sonicating tip under nitrogen protection. Finally, the desired quantity of $Pd(NO_3)_2$ solution was added. UV-visible spectroscopy measurements suggested that Pd was reduced and deposited exclusively by the GR reaction (Fig. 2a) and X-ray photoelectron spectroscopy confirmed the electronic transformation between the Pd and Cu atoms and formation of the alloy (Fig. 2b and c).

Also, Lucci *et al.* designed a PtCu SAA catalyst with a low concentration of individual Pt atoms by adding H_2PtCl_6 aqueous solution to a pre-reduced Cu/Al_2O_3 sample.[52] The reduction procedure was carried out under nitrogen protection with constant stirring. The EXAFS results showed the first shell interaction distance of 2.63 Å, which is between that of Pt–Pt (2.77 Å) and Cu–Cu (2.56 Å). In addition, no Pt–Pt bond existed. Thus, these results provide direct evidence for the presence of only Pt single atoms instead of clusters. In addition, the ACHAADF image also distinguished isolated Pt atoms on the Cu surface, also demonstrating the formation of the PtCu SAA structure (Fig. 2d–f).

Briefly, the displacement reaction between different types of metals provides an effective strategy for the synthesis of SAA catalysts. The GR process is a considerably facile and mild route without protective agents to fabricate SAA catalysts. Nevertheless, this route can only dissolve the less noble element and deposit the more noble one. Besides, the final structure of SAAs synthesized *via* the GR method is dependent on the shape and size of the host clusters/particles, which limits the application of the GR method.

In addition to the GR method, an NiCu SAA supported on SiO_2 was prepared *via* a modified electroless GR method,[54] according to the following redox reaction:

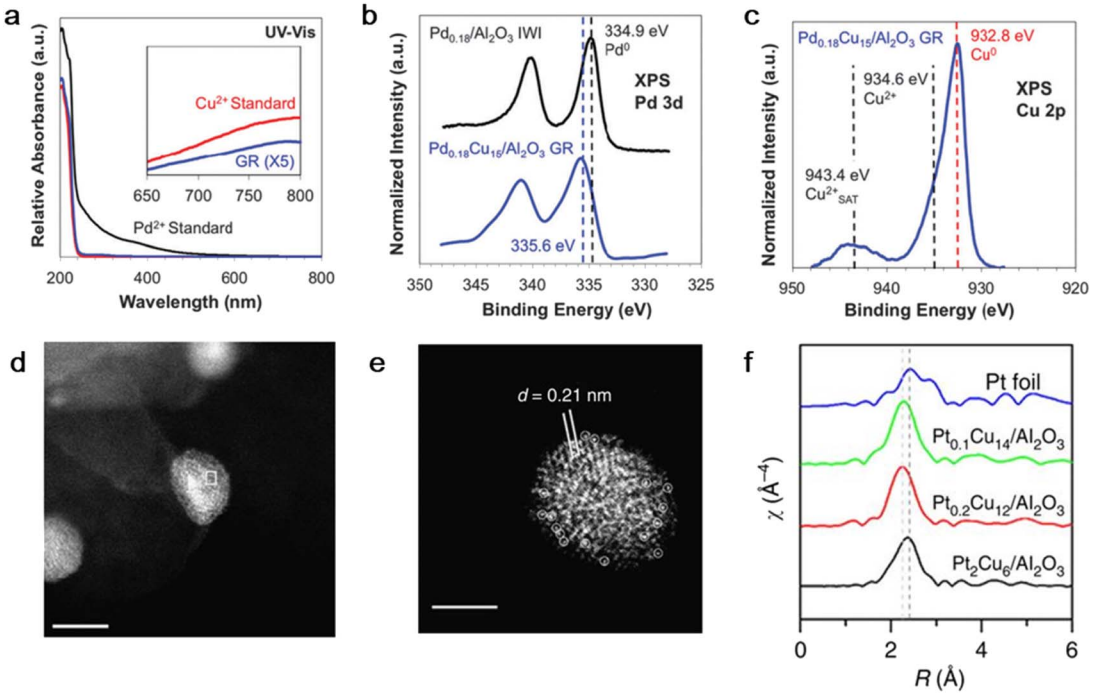

Fig. 2 (a) UV-vis spectroscopy, (b) Pd 3d XPS and (c) Cu 2p XPS of $Pd_{0.18}Cu_{15}/Al_2O_3$ prepared by GR method.[46] (d) and (e) HAADF-STEM images and (f) EXAFS k^3-weighted Fourier transforms of PtCu-SAA supported on γ-Al_2O_3.[53]

$$2Cu + 2OH^- + Ni^{2+} = Cu_2O + Ni + H_2O,\ \Delta E^0 = +0.103\ V \quad (2)$$

Similar to the above-mentioned GR method, the corresponding large potential difference guaranteed the deposition of Ni on the Cu_2O surface, which was spontaneously derived from the oxidation of the Cu metal in alkaline solution (OH^-). In detail, NaOH was mixed with the Ni precursor ($Ni(NO_3)_2 \cdot 6H_2O$) under an N_2 atmosphere followed by the addition of a certain amount of pre-reduced Cu/SiO_2 and continuous stirring. PtCu-SAA and PdCu-SAA were also obtained using this method.[54]

2.2.2 Successive reduction method. The successive reduction method is another step-wise reduction method, where first the metal ions are reduced into NPs, and then a reduction treatment is carried out. Similar with SAAs prepared *via* other methods, the guest metal is usually deposited on the surface of the host metal, presenting a core–shell structure. The successive reduction method does not involve the annealing process of GR reaction, avoiding the aggregation and growth of the guest metal atoms.

Toshima *et al.* fabricated a colloidal Au/Pd alloy with single Au atoms on the surface of Pd clusters *via* this effective and versatile tool with an average diameter of 1.5 nm (Fig. 3a and b).[55] Firstly, PVP-protected Pd clusters with ideal structure of Pd_{55} were prepared *via* the alcohol reduction method. Then, the desired amount of Au^{3+} with PVP aqueous solution was rapidly added to a mixture of Pd_{55} clusters and L-ascorbic acid. It should be noted that the reducibility of Pd is much weaker than that of L-ascorbic acid, and consequently Au^{3+} would react with L-ascorbic acid first. Thus, L-ascorbic acid enabled the *in situ* reduction of the Au^{3+} ions on the Pd_{55} surface, and finally the

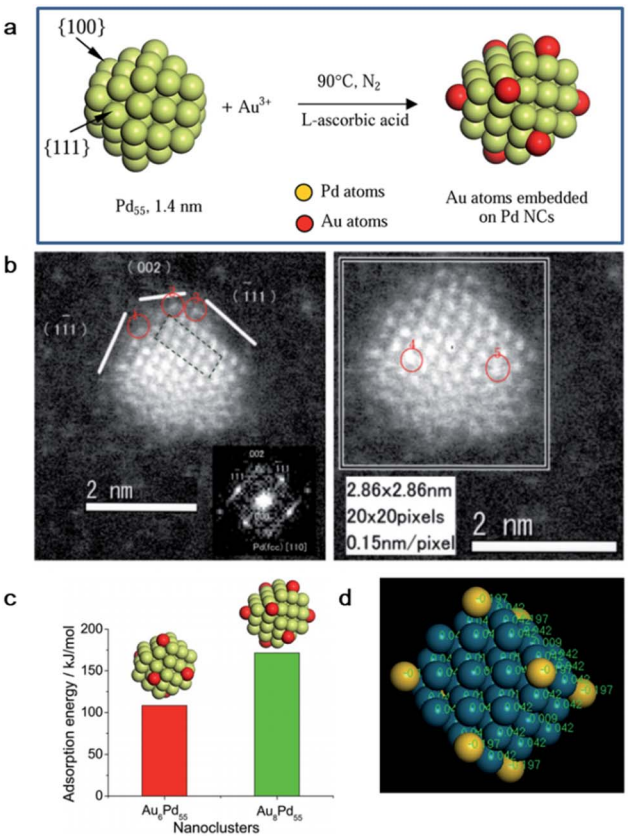

Fig. 3 (a) Schematic illustration and (b) HAADF-STEM image of AuPd SAA by the successive reduction method. (c) Adsorption energy of isolated Au atoms on Pd(110) and (111) plane. (d) Electronic structure of AuPd SAA calculated by DFT.[55]

formation of the AuPd alloy instead of Au nanoparticles. It is worth noting that heating the reaction temperature was performed quickly after L-ascorbic acid was added to prevent the galvanic replacement of Pd by Au^{3+}. For the obtained $Au_{55}Pd_{55}$, the deposition of Au atoms was indeed heterogeneous, where the center and edge Au accounted for 30% and 44% of all the metal atoms, respectively. Density function theory (DFT) calculation demonstrated that the Au atoms are preferentially located at the Pd(111) plane than that at the Pd(100) plane and coordinated by three Pd atoms (Fig. 3c). In addition, electronic charge transfer from the Pd to Au atoms also occurred, resulting in negatively charged Au atoms, while positive Pd atoms (Fig. 3d).

More importantly, the successive reduction method breaks the limits of the GR method of the dissolution of the less noble component and deposition of the more noble element. Different from that of the Au_3Pd_{55} SAA prepared by Toshima, a PdAu SAA structure was also constructed by alloying isolated Pd with Au clusters. Classically, Zhang *et al.* prepared PdAu-SAA with single Pd atoms *via* the facile successive reduction method, as follows: (i) $H_2N(CH_2)_3Si(OC_2H_5)_3$-functionalized silica gel (SiO_2-APTES) was firstly dispersed in $HAuCl_4$ solution, and then reduced by $NaBH_4$ to obtain supported Au particles and (ii) addition of $Pd(NO_3)_2$ solution with a certain concentration to the above-mentioned precipitate. The experimental and characterization results demonstrated that the absolute isolation of Pd by Au occurred under the preparation condition where the atom ratio of Pd/Au was less than 0.025 and the addition of Pd efficiently prevented the sintering of Au nanoparticles.[55]

Sykes *et al.* also synthesized $Pd_{0.02}Au_{0.98}$ NPs with an average diameter of 7.6 ± 1.9 nm *via* the successive reduction method.[21] During the preparation of the $Pd_{0.02}Au_{0.98}$ NPs (Fig. 4a), Au NPs were firstly synthesized using poly(vinylpyrrolidone) as protection and ethylene glycol as the reducing agent at 90 °C. After cooling to ambient temperature, $Pd(NO_3)_2 \cdot xH_2O$ was added, which was also reduced by ethylene glycol. They found that active site geometries in bimetallic alloys can be affected by CO and temperature treatment. In the case of the prepared $Pd_{0.02}Au_{0.98}$ NPs, the Pd single-atom phase could be transformed into clusters by changing the exposed CO partial pressure, as confirmed by the CO-DRIFTS results (Fig. 4b–g). During the ethanol dehydrogenation reaction, $Pd_{0.02}Au_{0.98}$ with Pd clusters leads to a range of products (including CO, ethyl acetate, and CH_4), while the $Pd_{0.02}Au_{0.98}$ SAA phase exhibited high selectivity for acetaldehyde and hydrogen.

2.3 Physical vapor deposition

Physical vapor deposition is the earliest method used to prepare SAA catalysts. In this method, the guest metal atoms are gasified

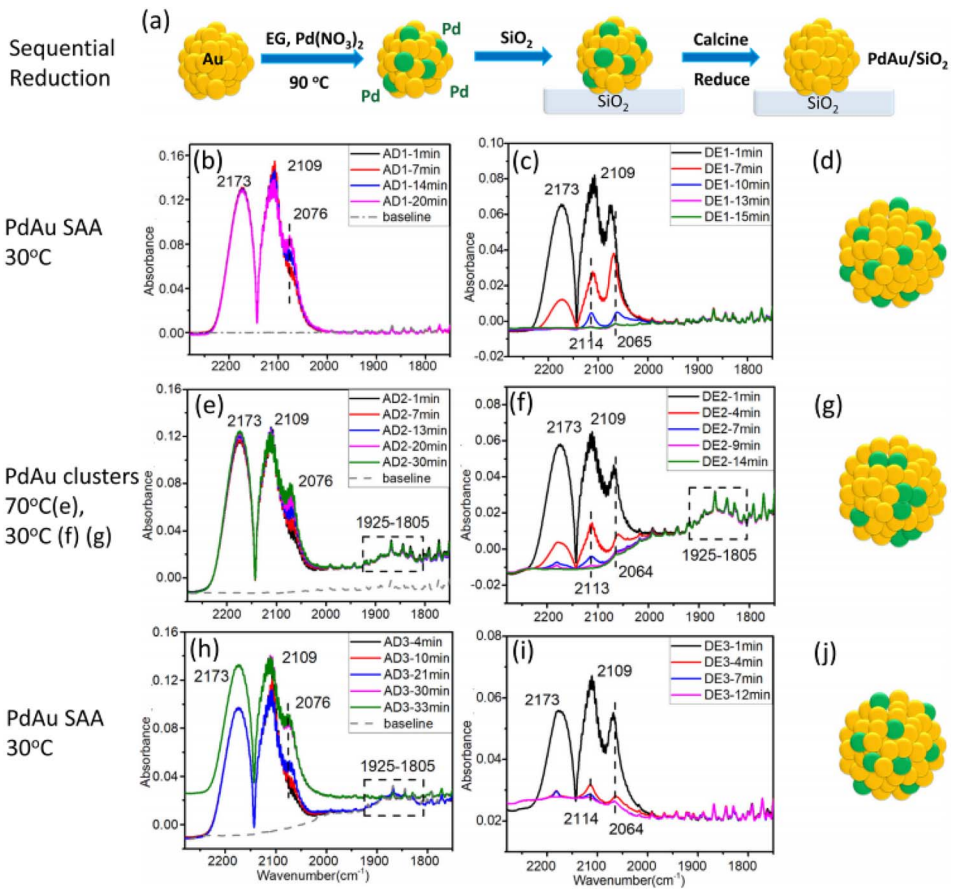

Fig. 4 (a) Schematic illustration and (b–j) CO-DRIFTS results and the corresponding structures of $PdAu/SiO_2$.[21]

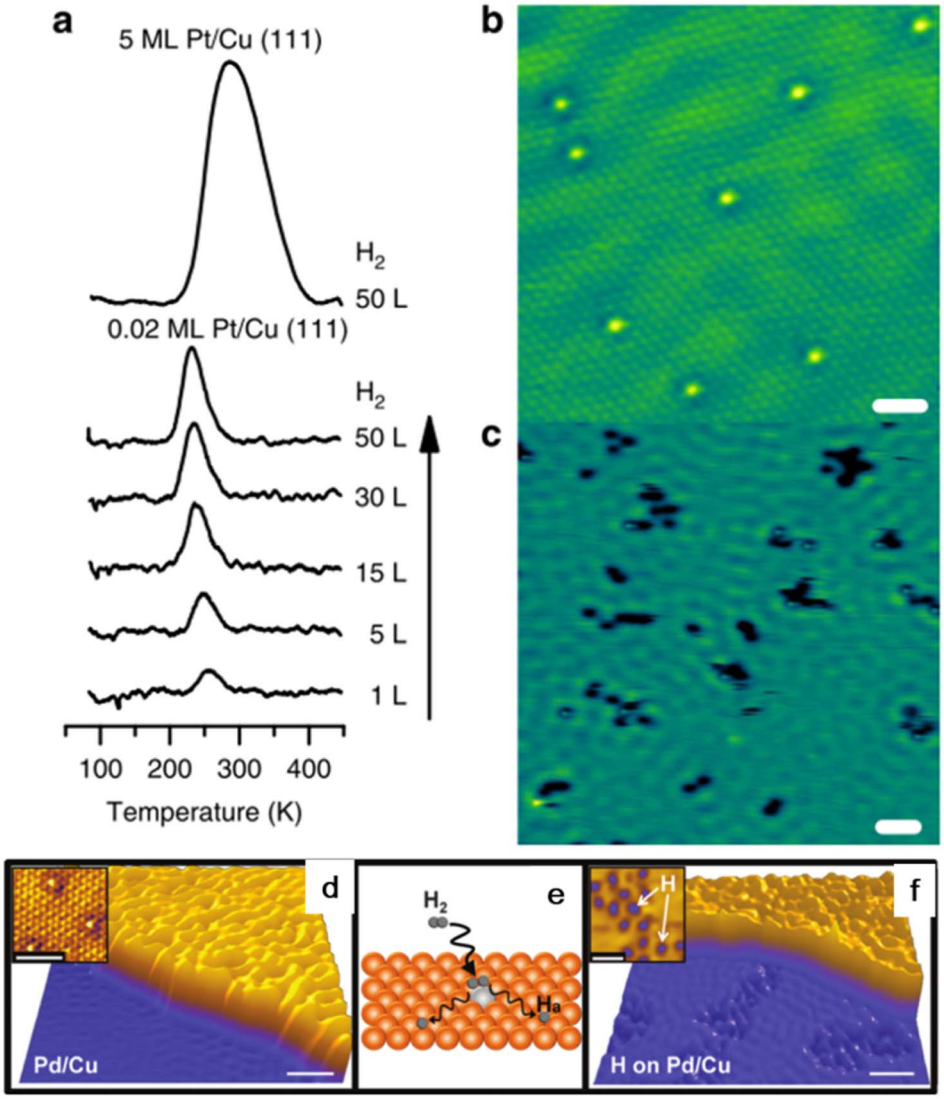

Fig. 5 (a) TPD traces of H_2 uptake, (b) STM image and (c) H_2 state on Pt/Cu(111) surface. (d and e) STM image of pristine PdCu(111) surface and (f) H_2 state on PdCu(111) surface.[53]

by physical methods under ultra-high vacuum (UHV) conditions, and then deposited on the surface of the host metal in the form of single atoms through the plasma process, thus forming solid deposits.[56] The research group led by Sykes successfully prepared PtCu, PdCu, PdAu and other SAA materials using this method.[12,57–59] Taking the preparation of the PtCu-SAA catalyst as an example, Cu(111) single crystals were firstly cleaned under ultrahigh vacuum using cycles of Ar^+ sputtering and annealing. Then, Pt was deposited onto the clean Cu(111) sample using an electron beam evaporator, allowing accurate and reproducible Pt surface coverage by varying the deposition time.[52] Consequently, the Pt atoms can be deposited on the surface step edge *via* place exchange and incorporated into the terraces directly. The STM image of PtCu demonstrated the existence of Pt on the Cu(111) surface as individual and isolated species, even at a higher local concentration near the step edge regions (Fig. 5a). In the case of the PtCu SAA, the Pt atoms act as the entrance and sites for H_2 dissociation and recombination (Fig. 5). The energy barrier of H_2 dissociative adsorption is negligible and the dissociated H atoms spill over from the Pt sites to the neighboring Cu atoms, allowing for an increase in weakly bound H on Cu.

Hannagan *et al.* studied the atomic-scale structure of Rh on Cu surface by developing an RhCu SAA UHV catalyst.[23] Studies on Rh/Cu(111) showed that the Rh atoms can alloy preferentially at the step edge in the isolated state and CO (common probe molecule) on the isolated Rh sites interacts *via* dipole–dipole coupling rather than chemical interactions. In the case of the isolated Pt alloyed SAA, the Pt atoms alloy directly in the terraces and regions near the step edges of Cu(111) and are randomly distributed throughout the surface.[60,61] The detailed investigation of the alloying process demonstrated that temperature control during the deposition plays a predominate role in maintaining the Pd atoms in the monodispersed state in the surface layer. The evaporated Pd atoms are adsorbed on the Cu surface and diffuse over the terraces randomly until they are

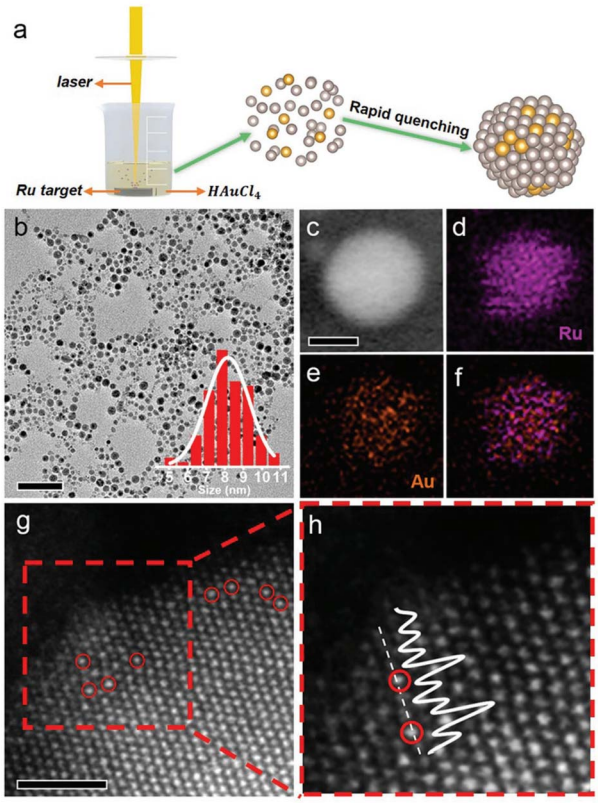

Fig. 6 (a) Schematic illustration, (b) TEM image and particle size distribution, (c–f) HAADF image and elemental mapping, and (g) and (h) atomic-resolution HAADF-STEM imaged of RuAu SAA prepared *via* the LAL method.[63]

trapped at the nearest ascending step edge, and then alloy into the Cu surface layer.[12]

Physical vapor deposition provides a synthetic strategy for better understanding the interaction between bimetals with precise coverage control by adjusting the flux of the guest metal or the deposition time. However, the cost of the equipment used in this method is very high and the yield is low, which limit its wide practical application in industry.

2.4 Laser ablation in liquid

Laser ablation in liquid (LAL) is a reliable method to synthesize SAA catalysts whose parent metals are immiscible in the solid state due to its strong quenching effect.[62] Du's group synthesized an RuAu SAA through the LAL technique in two steps, where the Ru target was firstly immersed in an HCl and $HAuCl_4$ mixed aqueous solution, and then irradiated by a nanosecond laser. The irritation process facilitated the vaporization of the Ru target and thermal decomposition of $HAuCl_4$, resulting in the formation of the RuAu SAA during the subsequent fast quenching. Further, the HAADF-STEM image revealed that the Au guest was individually dispersed in the Ru substrate and occupied the position of Ru atoms (Fig. 6).[63]

In conclusion, diverse methods for the synthesis of SAAs have been developed and reported, making the study of alloy catalysts at atomic precision become a hot topic in catalytic chemistry. The initial wet co-impregnation method, galvanic replacement method, successive reduction method and laser ablation in liquid for the synthesis of SAA catalysts have their own characteristics. However, based on the current controllable methods for the synthesis of SAA catalysts, the utilization efficiency of precious metal precursors is not high during the preparation process. Therefore, it is urgent to develop methods for the synthesis of SAA catalysts with the advantages of simple operation, large-scale synthesis, wide applicability, high atomic utilization rate and large loading capacity (Table 1).

3 Applications of SAA catalysts

Based on the strong theoretical foundation of science and advanced materials synthesis technology, it is possible to coordinate and isolate the guest metal atom with the host metal. Due to the different atomic radius, work function and negativity of the guest and host metal, the coordination environment of the guest atom changes and charge transfer occurs between the two metals after the formation of the SAA structure. Accordingly, the surface state density of the guest atom is affected by the host metal element, which tends to change the adsorption properties and dissociation ability of the substrate molecule and the intermediate species of the reaction.

Table 1 Summary of methods for the preparation of SAAs with their merits and demerits

Synthetic method	Samples	Merits	Demerits	Ref.
Initial wet co-impregnation	PtCu SAA PdAg SAA FePd SAA	Easy operation; low cost; facile process and no need for specific apparatus	Low yield and long synthesis cycle	39, 41 and 64
Galvanic replacement method	AgCu SAA PdCu SAA AuPd SAA	Special compositions and structures; long shelf life	Requires a difference in reduction potentials	65–67
Successive reduction method	AuPd SAA	Available complex structures; high catalytic activity	Complicated steps	55
Physical vapor deposition	PtCu(111) PdAu(111) PdAg(111)	Simple steps	High equipment cost and low yield	39, 52 and 60
Laser ablation in liquid	RuAu SAA	Simple operation	Low yield	63 and 68

Consequently, the catalytic performance of SAA catalysts can be adjusted and strengthened. Simultaneously, when the metal catalyst is decreased to the atomic level, its active sites and reaction paths of may change. In addition, the metal–metal interface between the isolated guest atoms and the host metals in SAAs may also lead to an enhanced catalytic performance. Therefore, SAA catalysts show superior catalytic activity to traditional mono-metallic catalysts due to their special geometrical structure and electronic properties. Studies on SAA catalyst are important in the development of heterogeneous catalysts at the atomic scale, which have become one of the future development directions of heterogeneous catalysts.[69] In this section, we summarize the applications of SAA materials in heterogeneous catalytic reactions, including selective hydrogenation, dehydrogenation, oxidation and hydrogenolysis reactions.

3.1 Selective hydrogenation reaction

The selective hydrogenation of unsaturated hydrocarbons is a basic process for the production of fine chemicals in the chemical industry, and in this case Pd-based catalysts have already demonstrated great catalytic activities.[70–73] However, traditional Pd nanoparticles can homogenize H_2 molecules into two H atoms, but the strong adsorption ability of Pd for H atoms is not conducive to the desorption of the H atoms, which limits the improvement in the catalytic efficiency of Pd catalysts for the hydrogenation reaction.[74,75] This issue is usually alleviated by Pd-based bimetallic catalysts with a precisely designed composition to retain high activity, while increasing selectivity.

Effective solutions for PdCu SAAs were first reported by Skykes and co-workers, where that individual, single Pd replaces the Cu element in the topmost surface layer (Fig. 7).[12] Due to its unique structure, the PdCu SAA possesses a bifunctional surface, which shows particular functions in the selective hydrogenation of styrene and acetylene. It was found that the dissociation barrier of H_2 on isolated Pd atoms is low and the dissociated H atom is weakly bounded. The dissociated H atoms spill over onto the neighboring Cu surface, and subsequently desorbed with low energy. Thus, facial hydrogen dissociation at the individual Pd site and weak binding to Cu sites guarantee the high activity and selectivity of the selective hydrogenation reaction. At present, it has been reported that PdAu, PdAg, PdCu, PtCu, NiIr and other SAA catalysts have been applied in the selective hydrogenation of olefins, acetylene, styrene, levulinic acid, and furfural and other reactions.[24,44,53,76–78]

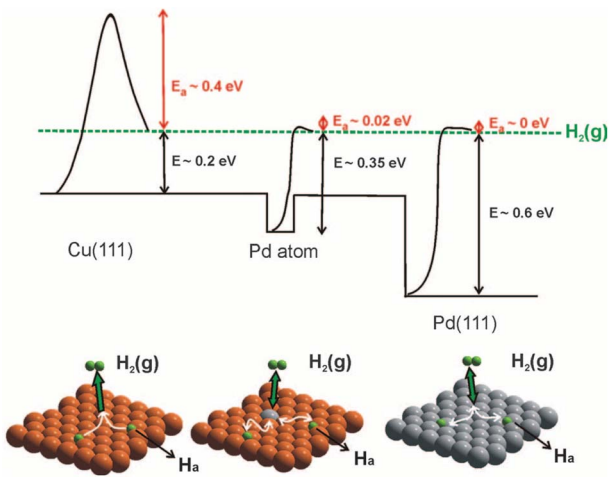

Fig. 7 H_2 potential dissociation energy and spillover process on Pd SAA, pure Cu(111) and Pd(111).[12]

Compared with the traditional Pd-based hydrogenation catalytic materials, PdCu SAA catalysts change the catalytic hydrogenation path due to the presence of bimetallic interfaces sites and improve the utilization of the precious metal Pd. Zhang *et al.* prepared an Ag-alloyed Pd SAA catalyst *via* the incipient wetness co-impregnation method to selectively hydrogenate acetylene to ethylene in an ethylene-rich stream.[41] It was found that single Pd-alloyed PdAg-SAA presented higher selectivity than that of the AuPd SAA. Even at a Pd loading as low as 168 ppm in AgPd-SAA, the catalyst still showed 92.6% conversion of acetylene and 92.3% ethylene selectivity, representing the best performance (85.5% yield) reported to date. This can be attributed to the geometric and electronic interactions between Pd and Ag, which altered the activation of acetylene and adsorption of the ethylene product.[43]

3.2 Dehydrogenation reaction

Recently, the development of shale gas has aroused the interest from researchers in C–H activation. Catalytic dehydrogenation through C–H activation is the most important step in the production of fine chemicals such as olefin from light alkenes.[79–81] Pt-based catalysts are the most frequently used catalysts for C–H activation, but it is easy to break the C–C bond, leading to carbon deposition and deactivation of the catalyst, and the high price of Pt metal prohibits its widespread use.[82,83] Thus, to solve this problem, Sykes proposed the strategy of using the PtCu SAA catalyst to facilitate C–H bond activation and avoid the formation of coke observed on clusters or particles. The present studies on alkanes related to C–H activation include methyl, methane and butane. These studies provide direct evidence from the determination of the catalytic active sites on the atomic scale, proof of the spillover intermediate products and the thermodynamics and kinetics of the reaction pathway.[60,84] It was found that the addition of Pt single atoms in PtCu-SAA can effectively facilitate C–H bond cleavage, and the activation temperature is 200 °C lower than that of the monometallic Cu catalyst under practical operation conditions (Fig. 8). The results are attributed to the intermediate barrier for C–H activation compared with pure metals and the endothermic process of dehydrogenated fragment formation. At present, alkenes dehydrogenated by SAA catalysts mainly include propane, ethanol, methanol, and formic acid and the commonly used SAA catalysts are mainly PtCu, PdCu and NiCu SAA.[54,84–88]

SAA catalysts not only promote C–H activation but also avoid the formation of coke on large ensembles.[89] In the terms of propane dehydrogenation (PDH), this reaction is normally

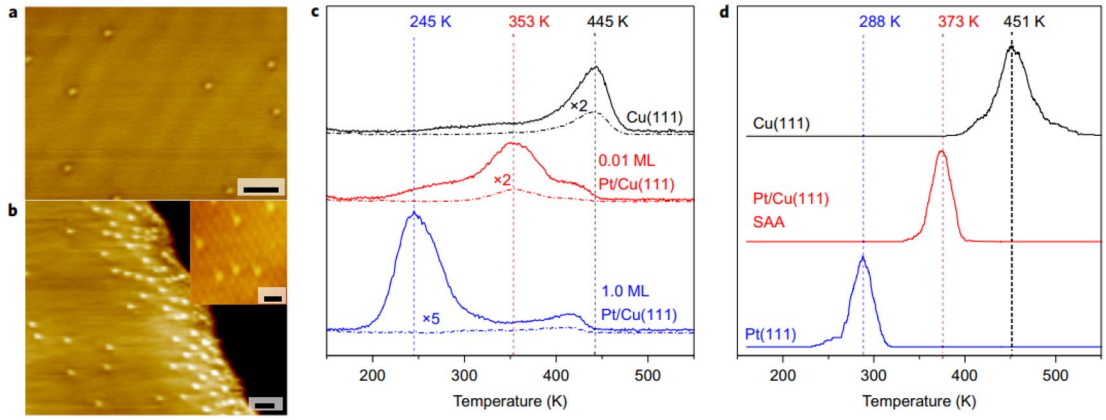

Fig. 8 (a) and (b) STM images of Pt/Cu(111) SAA surface. (c) TPR traces and (d) simulated TPR of methane evolution.[60]

catalyzed by PtM alloys, where M represents 3d and/or 4d transition metals, including Sn, Zn, Ga, In, Ge and Cu. However, previous studies found that these PtM alloys are restricted by the scaling relationship. When the energy barrier of propane dehydrogenation is lower (*i.e.*, higher activity) for PtM alloy catalysts, the interaction between C and Pt is stronger, resulting in the stronger adsorption of the product (propylene) and deeper dehydrogenation (*i.e.*, lower activity). Different from the conventional PtM alloy catalysts, SAA catalysts with nanoparticles, metals or model surfaces hosting isolated atoms on their surface can avoid the linear scaling relationships and allow for the rational fine-turning of activity and selectivity during PDH.

Gong *et al.* firstly certified by DFT calculations that there is a considerable negative difference between the desorption energy of propane and further dehydrogenation barrier of the target product propylene for PtCu SAA, whilst the dehydrogenation energy barrier of propane is also maintained properly. Then, they further prepared PtCu SAA supported on γ-Al_2O_3 *via* an atomic dilution method to confirm the above-mentioned conclusion that PtCu SAA are indeed capable of breaking the restriction of the PtM alloy scaling relationship (Fig. 9). The PtCu SAA with a low

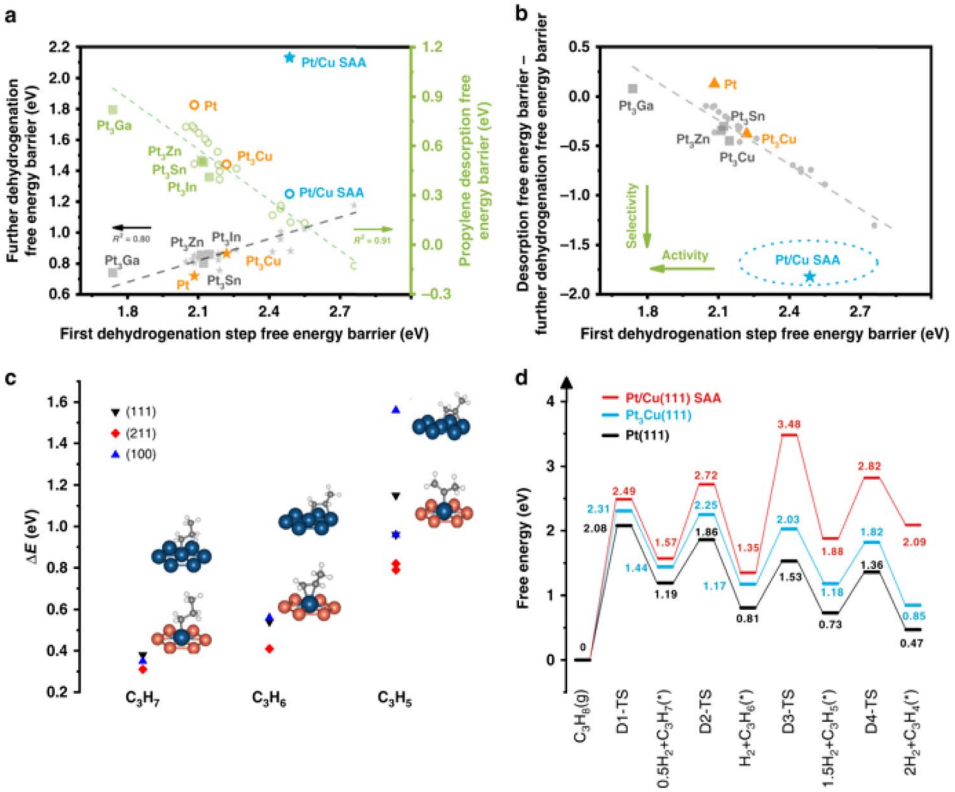

Fig. 9 (a) Scaling relationship between first dehydrogenation barrier and propylene desorption barrier/deep dehydrogenation barrier. (b) Screening of Pt-based bimetallic catalyst for PDH. (c) Binding energy difference and structures (on (111) surface only) of dehydrogenated intermediates C_3H_x ($x = 7$, 6, 5) over pure Pt surface and Pt/Cu SAA surface. (d) Energy profiles of PDH over Pt/Cu SAA, $Pt_3Cu(111)$ and Pt(111).[39]

loading of Pt (0.1 wt%) showed a high formation rate of 10.6 mol g_{Pt}^{-1} h^{-1} with high propylene selectivity (~90%) under atmospheric pressure and high temperature (520 °C). They further performed DFT calculations by constructing 54 reversible reaction steps and kinetic Monte Carlo simulations to compare the PDH performance and coke formation on the PtCu SAA catalyst and that on pristine Pt catalysts.[90] Three reasons were proposed to explain the better performance on the PtCu SAA catalysts than pure Pt, *i.e.*, the energy barrier of C–C bond cracking is much larger on Pt catalysts, whist the energy barrier of C–H cleavage on the two catalysts is the same; the deep dehydrogenation of propene is attributed to the smaller frequency of the forward step; and the main coke species for the PtCu SAA catalyst changes compared with Pt.

Furthermore, to solve the agglomeration of Cu particles under high temperature, $CuSiO_3$ was selected as a support for PtCu SAAs.[91] The evaluation results confirmed that the optimized PtCu SAA catalyst supported on $CuSiO_3$ still achieved above 42% propane conversion and 93% propylene selectivity at 580 °C after 30 h PDH reaction. In addition, Hannagan *et al.* performed first-principle calculations and suggested that individual Ru atoms embedded in a Cu(111) surface should be stable and efficient to converse propane to propene with high selectivity and resistance to coke formation.[22]

3.3 Oxidation reaction

Selective oxidation is an effective way to prepare high-value-added chemicals. Au catalysts are among the most commonly used catalysts in oxidation reactions.[92] It has been reported that compared with single-type Au active sites, catalysts containing multiple active sites such as bimetallic alloys are preferred due to their better activity and selectivity.[93,94] Cargnello *et al.* synthesized a PdAu-SAA catalyst and studied its structure–activity relationship in the selective oxidation of 2-peopanal to acetone.[95] They found that the introduction of Pd single atoms with a low concentration (1.4 at%) in Au catalysts could greatly improve the catalytic performance compared with Pd or Au individually. Pd single atoms are mainly used to dissociate H_2 molecules, while the Au-oxide interface is necessary to adsorb O_2 molecules without dissociation, and the two species enable the generation of selective oxidized species. The synergistic effects between single Pd and Au are responsible for the formation of reactive oxidizing species and limiting oxygen dissociation, enabling the selective oxidation and complete combustion. Toshima *et al.* developed crown jewel-structured Au/Pd catalysts *via* the GR reaction method, where Au atoms were atomically dispersed on the top sites of Pd nanoclusters.[68,96] The obtained surface Au atom-decorated Pd SAA catalysts presented 20–30 times higher activity than that of Au particles with a size of 1.4 nm diameter during glucose oxidation, which can be associated with the high negative charge of the Au atoms and their unique structure caused by tuning the number of Pd atoms.

In addition to Au and Pd-based SAA catalysts, it has been reported that PtRh, AgCu and AgCu SAA catalysts are used for ethanol oxidation, NiPt, PdCu and PtRu SAA are used for methane oxidation, PdCu and PdBi SAA catalysts are used for methanol oxidation, and AuPd- and Ni-based SAA catalysts are used for carbon monoxide oxidation.[97–106] For example, a single Ni atom-alloyed Pt SAA supported on porous graphdiyne presented excellent catalytic activity and durability towards methanol oxidation.[107] The low valence state of Pt in NiPt SAA is the origin of its activity and the high resistance to CO poisoning. In addition, PdCu SAA catalysts prepared by galvanic replacement method are being studied as selective catalysts for the oxidation of methanol to methyl formate at low temperatures by Stephanopoulos. The single Pd atoms in the Cu matrix are confirmed to be oxidized locally and the presence of Pd oxide species increases the activity, selectivity and stability.

Li *et al.* constructed two examples of Pd/Cu(111) SAAs with Pd atoms adsorbed and doped on Cu(111) surface, respectively (Fig. 7).[108] They calculated the energies for the different reaction paths for CH_4 partial oxidation using these two SAA catalysts examples. The calculation results indicated that oxygen as the oxidant is more preferable than hydroxy to reduce the activation energy barrier of CH_x oxidation. However, the process of partial methane oxidation on the two Pd/Cu(111) samples are different, as follows: ($CH_4 \rightarrow CH_3 \rightarrow CH_3O \rightarrow CH_2O \rightarrow CHO \rightarrow CO$) on doped Pd/Cu(111) with the activation energy of 1.46 eV, while $CH_4 \rightarrow CH_3 \rightarrow CH_2 \rightarrow CH \rightarrow CHO \rightarrow CO$ on adsorbed Pd/Cu(111) surface with the activation energy of 1.49 eV. Thus, it can be concluded that doped Pd/Cu(111) is more favorable to generate CO and shows better performance in terms of thermodynamics and higher capacity for sintering resistance.

Preferential oxidation of CO was investigated on the $Pt_{0.1}Cu_{0.19}/CeO_2$ catalyst by Wang *et al.* They found that the alloy with single dispersed Pt atoms showed higher catalytic activity than that of monometallic counterparts and the alloy with single dispersed Pt atoms was more stable than that with Pt–Pt bonds.[109] $PtCu_x$ SAA and copper-ceria interface are the main two types of active sites, which show a synergistic effect during catalysis. The DFT calculations and XPS results confirmed that Cu can partially transfer electrons to Pt *via* Pt–Cu bonds and the electronic interaction tuned the electronic structure of the PtCu SAA catalyst, which is responsible for the promotion of CO desorption, and finally improved the catalytic activity.

3.4 Hydrogenolysis reaction

Thus far, only PtCu SAA catalysts have been used for hydrogenolysis reactions, including hydrogenolysis of methyl glycolate to ethanol and hydrogenolysis of glycerol to 1,2-propanediol. Zhang *et al.* prepared the 0.1Pt–Cu/SiO_2 SAA, where Pt was isolated as single atoms and formed the Pt–Cu alloy phase.[65] They found that only 0.1 wt% isolated Pt with the surrounding Cu atoms improved the dispersion of Cu, increased the Cu^+/Cu^0 ratio and enhanced hydrogen activation without causing the C–C cleavage side reaction. Consequently, PtCu-SAA catalysts afford a reduced reaction temperature, unique ethanol selectivity as high as 76.7% and promising stability of over a 700 h time on stream in the methyl glycolate reaction.

The PdNi SAA with isolated Pd atoms dispersed on Ni nanoclusters breaks the strong metal-selectivity relations and

Table 2 Summary of the application of SAAs in heterogeneous catalytic reactions

Catalysts	Synthetic method	Reaction type	Catalytic activity	Ref.
PdCu SAA	Physical vapor deposition	Hydrogenation of styrene	Conversion: 80% Selectivity: 38%	12
PdCu SAA	Physical vapor deposition	Hydrogenation of acetylene	Conversion: 90% Selectivity: 33%	12
PdCu SAA	Galvanic replacement method	Hydrogenation of furfural	Conversion: 40.1% Selectivity: 99.1%	44
PtCu SAA	Galvanic replacement method	Hydrogenation of 1,3-butadiene	Conversion: 100% Selectivity: 100%	53
NiIr SAA	Sequential impregnation and reduction	Hydrogenation of styrene	Conversion: >99.9% Selectivity: >99.9%	112
AgPd SAA	Incipient wetness co-impregnation method	Hydrogenate acetylene	Conversion: 92.6 Selectivity: 92.3 Yield: 85.5%	43
PdNi SAA	Combining wet chemistry and ALD	Hydrogenation of nitriles	Yield:97%	110
PtCu SAA	Physical vapor deposition	Formic acid dehydrogenation	Conversion: 100% Selectivity: 100%	84
PtCu SAA	Incipient wetness co-impregnation method	Propane dehydrogenation	TOF: 10.6 mol g_{Pt}^{-1} h^{-1} Selectivity: 90%	39
PtSn SAA	Impregnation and calcination	Propane dehydrogenation	Productivity: 11.1 $mol_{C_3H_6}$ g_{Pt}^{-1} h^{-1}	113
PtCu SAA	Impregnation method	Propane dehydrogenation	Conversion: 42% Selectivity: 93%	91
PdCu SAA	Galvanic replacement method	Ethanol dehydrogenation	Selectivity: 100%	54
PtCu SAA	Galvanic replacement method	Ethanol dehydrogenation	Selectivity: 100%	54
PdCu SAA	Galvanic replacement method	Oxidation of methanol	Conversion: 32% Selectivity: 97%	101
PdBi SAA	Co-incipient wetness impregnation	Low temperature CO oxidation	Conversion: 100%	114
PtCu SAA	Galvanic replacement method	Hydrogenolysis of glycerol	Conversion: 99.6%% Selectivity: 99.2% TOF: 2.6×10^3 $mol_{glycerol}$ $mol_{PtCu-SAA}^{-1}$ h^{-1}	38
PtCo SAA	Ball milling approach	Hydrodeoxygenation of 5-hydroxymethylfurfural	Conversion: 100%% Selectivity: 92.9%	111

exhibits super catalytic performances with excellent recyclability in the hydrogenation of benzonitrile toward dibenzylamine.[110] Remarkably, PdNi SAA showed reaction activity of 8 and 4-times higher than that of the monometallic Pd and Pt standard catalysts, respectively, and the yield of dibenzylamine reached up to 97% under mild conditions. The DFT results confirmed that the synergistic effect in the PdNi SAA changed the reaction pathway from primary amines on Pd to the exclusive formation of secondary amines, which is responsible for the outstanding performance.

The hydrogenation of biomass-derived 5-hydroxymethylfurfural (HMF) into high-quality biofuel, *i.e.*, 2,5-dimethylfuran (DMF), is significant for the utilization of biomass. In this case, the PtCo SAA catalyst with Pt atoms fabricated by Ji *et al.* showed an excellent catalytic performance and stability for the hydrogenolysis of DMF to DHMF.[111] Single Pt atom electronic transfer to the Co atoms formed the $Pt^{\delta-}$–$Co^{\delta+}$ active site, which enhanced the C–O bond adsorption and decreased the adsorption of furan, resulting in improved catalytic selectivity and activity.

Our group also reported the preparation of a PtCu SAA with single Pt atoms dispersed on Cu nanoclusters.[38] Both the *in situ* experimental studies and DFT results confirmed that the Pt–Cu interfacial sites are the intrinsic active sites, where the single Pt atom promotes the dissociation of the central C–H, while the adjacent Cu atom is responsible for the terminal C–O bond breakage and adsorption. Compared with Pt nanoparticles, the synergistic SAA interfacial sites change the reaction pathway with a lower activity energy and boosted the performance of hydrogenolysis of glycerol to 1,2-propanediol with 98.8% yield (Table 2).

4 Conclusions and perspectives

In summary, single-atom alloy (SAA) catalysts contain an atomically dispersed metal and form an alloy phase. SAA catalysts significantly improves the utilization of noble metal and shows certain advantages in the field of heterogeneous catalysis. SAA catalysts have been prepared *via* initial wet impregnation, physical vapor deposition and laser ablation in liquid technique method. SAA catalysts make full use of noble metal atoms and maximize the alloy metal sites to enhance the catalytic activity and selectivity. Normally, the synergistic effects and the interaction between the host and guest metals in SAAs afford remarkable catalytic performances and the stability of atomic-level dispersed noble metals under harsh reaction conditions. Furthermore, the electronic and geometric effects of SAA change the reaction pathway and lower the activation energy, thus affecting the overall activity and selectivity. Also, the unique features of SAA can break the liner scaling

relationships caused by the activation of the reactants and weak binding of the intermediates. Further, designing efficient SAA catalysts with clear and uniform structure provide a strategy to identify active sites, establish the reaction mechanisms and investigate structural changes in the active sites during the full reaction process from the investigation of surface science, theoretical calculations and catalytic studies. SAAs exhibit excellent performances in many heterogeneous catalytic reactions, such as selective hydrogenation, dehydrogenation, oxidation reactions and hydrogenolysis reactions.

Although remarkable progress has been achieved in both the preparation methods and application of SAAs, there still are many issues that need to be addressed in the field of heterogeneous catalysis using SAA catalyst, as follows: (1) to ensure the isolated state of the guest metal without agglomeration during the preparation and catalytic reaction, the loading of SAA guest molecules is generally relatively low (normally less than 0.5%), which is not conducive to their characterization, and also brings great difficulties and challenges in actual industrial production. Therefore, there is an urgent need to develop methods for the preparation of SAA catalysts with large guest metal loadings. (2) There are many types of SAA catalyst systems, but each SAA catalyst is not the same in terms of chemical nature. Thus, more in-depth studies on the electronic properties and catalytic mechanism using different experimental and theoretical methods need to be carried out to understand the catalytic performance. (3) SAA catalysts contain not only a special structure of monatomic guests, but also a bimetallic alloy structure, and consequently their catalytic mechanism is different from the traditional mechanism. However, the development of new methods and theories to reveal the catalytic mechanism of SAAs is a challenge at present.

Overall, due to their special geometric and electronic structures, SAA catalysts will attract increasing attention. There are opportunities and challenges in the exploration of potential SAAs in the field of heterogeneous catalysis in the future. With the development of surface science, theoretical simulation and other technologies, the current problems will be solved and SAAs will be applied in more fields. We hope that this review offers a good overview for better understanding the synthetic strategies, catalytic properties, catalytic design and further heterogeneous catalytic applications of SAAs.

Author contributions

Shuang Zhang wrote the original draft of this manuscript. Ruiying Wang is responsible for drawing the pictures. Hua Zhao planned and directed the project. Xi Zhang designed this work. All authors contributed to the discussion of this study and reviewed this manuscript.

Conflicts of interest

The authors declare no known competing financial interests or personal relationships that could have appeared to influence the work reported in this work.

Acknowledgements

This work was supported by R&D Program of Beijing Municipal Education Commission (KM202210011005) and Research Foundation for Youth Scholars of Beijing Technology and Business University (QNJJ2020-26) unveiled the project.

References

1 J. D. Lee, J. B. Miller, A. V. Shneidman, L. Sun, J. F. Weaver, J. Aizenberg, J. Biener, J. A. Boscoboinik, A. C. Foucher, A. I. Frenkel, J. E. S. van der Hoeven, B. Kozinsky, N. Marcella, M. M. Montemore, H. T. Ngan, C. R. O'Connor, C. J. Owen, D. J. Stacchiola, E. A. Stach, R. J. Madix, P. Sautet and C. M. Friend, Dilute Alloys Based on Au, Ag, or Cu for Efficient Catalysis: From Synthesis to Active Sites, *Chem. Rev.*, 2022, **122**(9), 8758–8808.

2 M. Zhou, C. Li and J. Fang, Noble-Metal Based Random Alloy and Intermetallic Nanocrystals: Syntheses and Applications, *Chem. Rev.*, 2021, **121**(2), 736–795.

3 A. S. Rosen, S. Vijay and K. A. Persson, Free-atom-like d states beyond the dilute limit of single-atom alloys, *Chem. Sci.*, 2023, **14**(6), 1503–1511.

4 Q. Du, L. Huang, J. Fu, Y. Cao, X. Xing and J. Zhao, Single atom alloy clusters $Ag_{n-1}X$ (X = Cu, Au; n=7-20) reacting with O_2: Symmetry-adapted orbital model, *J. Chem. Phys.*, 2023, **158**(1), 014306.

5 C. Du, J. P. Mills, A. G. Yohannes, W. Wei, L. Wang, S. Lu, J.-X. Lian, M. Wang, T. Guo, X. Wang, H. Zhou, C.-J. Sun, J. Z. Wen, B. Kendall, M. Couillard, H. Guo, Z. Tan, S. Siahrostami and Y. A. Wu, Cascade electrocatalysis via AgCu single-atom alloy and Ag nanoparticles in CO_2 electroreduction toward multicarbon products, *Nat. Commun.*, 2023, **14**(1), 6142.

6 R. Patil, T. Dey, L. Kang, S. Liu, S. C. Jun and S. Dutta, Electronic and Structural Engineering of Atomically Dispersed Isolated Single-Atom and Alloy Architectures, *Small*, 2023, **19**(29), 2301675.

7 T. Zhang, A. G. Walsh, J. Yu and P. Zhang, Single-atom alloy catalysts: structural analysis, electronic properties and catalytic activities, *Chem. Soc. Rev.*, 2021, **50**(1), 569–588.

8 X.-F. Yang, A. Wang, B. Qiao, J. Li, J. Liu and T. Zhang, Single-Atom Catalysts: A New Frontier in Heterogeneous Catalysis, *Acc. Chem. Res.*, 2013, **46**(8), 1740–1748.

9 Z. Li, Y. Chen, S. Ji, Y. Tang, W. Chen, A. Li, J. Zhao, Y. Xiong, Y. Wu, Y. Gong, T. Yao, W. Liu, L. Zheng, J. Dong, Y. Wang, Z. Zhuang, W. Xing, C.-T. He, C. Peng, W.-C. Cheong, Q. Li, M. Zhang, Z. Chen, N. Fu, X. Gao, W. Zhu, J. Wan, J. Zhang, L. Gu, S. Wei, P. Hu, J. Luo, J. Li, C. Chen, Q. Peng, X. Duan, Y. Huang, X.-M. Chen, D. Wang and Y. Li, Iridium single-atom catalyst on nitrogen-doped carbon for formic acid oxidation synthesized using a general host-guest strategy, *Nat. Chem.*, 2020, **12**(8), 764–772.

10 W. Xie, H. Li, G. Cui, J. Li, Y. Song, S. Li, X. Zhang, J. Y. Lee, M. Shao and M. Wei, NiSn Atomic Pair on an Integrated

Electrode for Synergistic Electrocatalytic CO2 Reduction, *Angew. Chem., Int. Ed.*, 2021, **60**, 7382–7388.

11 X. Li, X. Yang, Y. Huang, T. Zhang and B. Liu, Supported Noble-Metal Single Atoms for Heterogeneous Catalysis, *Adv. Mater.*, 2019, **31**(50), 1902031.

12 G. Kyriakou, M. B. Boucher, A. D. Jewell, E. A. Lewis, T. J. Lawton, A. E. Baber, H. L. Tierney, M. Flytzani-Stephanopoulos and E. C. H. Sykes, Isolated Metal Atom Geometries as a Strategy for Selective Heterogeneous Hydrogenations, *Science*, 2012, **335**(6073), 1209–1212.

13 J. Zhao, J. Liu, Z. Li, K. Wang, R. Shi, P. Wang, Q. Wang, G. I. N. Waterhouse, X. Wen and T. Zhang, Ruthenium-cobalt single atom alloy for CO photo-hydrogenation to liquid fuels at ambient pressures, *Nat. Commun.*, 2023, **14**(1), 1909.

14 C. Du, S. Lu, J.-A. Wang, X. Wang, M. Wang, H. M. Fruehwald, L. Wang, B. Zhang, T. Guo, J. P. Mills, W. Wei, Z. Chen, Y. Teng, J. Zhang, C.-J. Sun, H. Zhou, R. D. L. Smith, B. Kendall, G. Henkelman and Y. A. Wu, Selectively Reducing Nitrate into NH_3 in Neutral Media by PdCu Single-Atom Alloy Electrocatalysis, *ACS Catal.*, 2023, **13**(16), 10560–10569.

15 M. Zhong, J. Zhao, Y. Fang, D. Wu, L. Zhang, C. Du, S. Liu, S. Yang, S. Wan, Y. Jiang, J. Huang and H. Xiong, Depositing Pd on the outmost surface of Pd1Ni/SiO2 single-atom alloy via atomic layer deposition for selective hydrogenation of acetylene, *Appl. Catal., A*, 2023, **662**, 119288.

16 Z. Xu, Z. Ao, M. Yang and S. Wang, Recent progress in single-atom alloys: Synthesis, properties, and applications in environmental catalysis, *J. Hazard. Mater.*, 2022, **424**, 127427.

17 J. Han, J. Lu, M. Wang, Y. Wang and F. Wang, Single Atom Alloy Preparation and Applications in Heterogeneous Catalysis, *Chin. J. Chem.*, 2019, **37**(9), 977–988.

18 H. Thirumalai and J. R. Kitchin, Investigating the Reactivity of Single Atom Alloys Using Density Functional Theory, *Top. Catal.*, 2018, **61**(5–6), 462–474.

19 D. A. Patel, G. Giannakakis, G. Yan, H. T. Ngan, P. Yu, R. T. Hannagan, P. L. Kress, J. Shan, P. Deshlahra, P. Sautet and E. C. H. Sykes, Mechanistic Insights into Nonoxidative Ethanol Dehydrogenation on NiCu Single-Atom Alloys, *ACS Catal.*, 2023, **13**(7), 4290–4303.

20 R. T. Hannagan, G. Giannakakis, M. Flytzani-Stephanopoulos and E. C. H. Sykes, Single-Atom Alloy Catalysis, *Chem. Rev.*, 2020, **120**(21), 12044–12088.

21 M. Ouyang, K. G. Papanikolaou, A. Boubnov, A. S. Hoffman, G. Giannakakis, S. R. Bare, M. Stamatakis, M. Flytzani-Stephanopoulos and E. C. H. Sykes, Directing reaction pathways via in situ control of active site geometries in PdAu single-atom alloy catalysts, *Nat. Commun.*, 2021, **12**(1), 1549.

22 R. T. Hannagan, G. Giannakakis, R. Reocreux, J. Schumann, J. Finzel, Y. Wang, A. Michaelides, P. Deshlahra, P. Christopher, M. Flytzani-Stephanopoulos, M. Stamatakis and E. C. H. Sykes, First-principles design of a single-atom-alloy propane dehydrogenation catalyst, *Science*, 2021, **372**(6549), 1444.

23 R. T. Hannagan, D. A. Patel, L. A. Cramer, A. C. Schilling, P. T. P. Ryan, A. M. Larson, V. Cinar, Y. Wang, T. A. Balema and E. C. H. Sykes, Combining STM, RAIRS and TPD to Decipher the Dispersion and Interactions Between Active Sites in RhCu Single-Atom Alloys, *ChemCatChem*, 2020, **12**(2), 488–493.

24 A. M. Alamer, M. Ouyang, F. H. Alshafei, M. A. Nadeem, Y. Alsalik, J. T. Miller, M. Flytzani-Stephanopoulos, E. C. H. Sykes, V. Manousiouthakis and N. M. Eagan, Design of Dilute Palladium-Indium Alloy Catalysts for the Selective Hydrogenation of CO2 to Methanol, *ACS Catal.*, 2023, **13**(15), 9987–9996.

25 J. S. Jirkovsky, I. Panas, E. Ahlberg, M. Halasa, S. Romani and D. J. Schiffrin, Single atom hot-spots at Au-Pd nanoalloys for electrocatalytic H_2O_2 production, *J. Am. Chem. Soc.*, 2011, **133**(48), 19432–19441.

26 M. T. Greiner, T. E. Jones, S. Beeg, L. Zwiener, M. Scherzer, F. Girgsdies, S. Piccinin, M. Armbruester, A. Knop-Gericke and R. Schloegl, Free-atom-like d states in single-atom alloy catalysts, *Nat. Chem.*, 2018, **10**(10), 1008–1015.

27 T. D. Spivey and A. Holewinski, Selective Interactions between Free-Atom-like d-States in Single-Atom Alloy Catalysts and Near-Frontier Molecular Orbitals, *J. Am. Chem. Soc.*, 2021, **143**(31), 11897–11902.

28 S. Nigam and C. Majumder, Single atom alloy catalyst for SO_3 decomposition: enhancement of platinum catalyst's performance by Ag atom embedding, *Nanoscale*, 2018, **10**(44), 20599–20610.

29 H. Wang, J. Li, M. Huang, J. Cui, Z. Cheng, R. Yu and H. Zhu, Single-atom alloys prepared by two-step thermal evaporation, *Nano Res.*, 2023, DOI: **10.1007/s12274-023-6146-4**.

30 N. Hopper, T. Thuening, S. Manzi, M. Weinert and W. T. Tysoe, Binding of Oxygen on Single-Atom Sites on Au/Pd(100) Alloys with High Gold Coverages, *J. Phys. Chem. C*, 2021, **125**(18), 9715–9729.

31 J. Choi, S. Seo, M. Kim, Y. Han, X. Shao and H. Lee, Relationship between Structure and Performance of Atomic-Scale Electrocatalysts for Water Splitting, *Small*, 2023, 2304560.

32 Q. Fu and Y. Luo, Catalytic Activity of Single Transition-Metal Atom Doped in Cu(111) Surface for Heterogeneous Hydrogenation, *J. Phys. Chem. C*, 2013, **117**(28), 14618–14624.

33 P. Aich, H. Wei, B. Basan, A. J. Kropf, N. M. Schweitzer, C. L. Marshall, J. T. Miller and R. Meyer, Single-Atom Alloy Pd–Ag Catalyst for Selective Hydrogenation of Acrolein, *J. Phys. Chem. C*, 2015, **119**(32), 18140–18148.

34 M.-J. Cheng, E. L. Clark, H. H. Pham, A. T. Bell and M. Head-Gordon, Quantum Mechanical Screening of Single-Atom Bimetallic Alloys for the Selective Reduction of CO2 to C1 Hydrocarbons, *ACS Catal.*, 2016, **6**(11), 7769–7777.

35 X. Chang, Z.-J. Zhao, Z. Lu, S. Chen, R. Luo, S. Zha, L. Li, G. Sun, C. Pei and J. Gong, Designing single-site alloy catalysts using a degree-of-isolation descriptor, *Nat. Nanotechnol.*, 2023, **18**(6), 611–+.

36 G. Giannakakis, P. Kress, K. Duanmu, H. T. Ngan, G. Yan, A. S. Hoffman, Z. Qi, A. Trimpalis, L. Annamalai, M. Ouyang, J. Liu, N. Eagan, J. Biener, D. Sokaras, M. Flytzani-Stephanopoulos, S. R. Bare, P. Sautet and E. C. H. Sykes, Mechanistic and Electronic Insights into a Working NiAu Single-Atom Alloy Ethanol Dehydrogenation Catalyst, *J. Am. Chem. Soc.*, 2021, **143**(51), 21567–21579.

37 G. Giannakakis, M. Flytzani-Stephanopoulos and E. C. H. Sykes, Single-Atom Alloys as a Reductionist Approach to the Rational Design of Heterogeneous Catalysts, *Acc. Chem. Res.*, 2019, **52**(1), 237–247.

38 X. Zhang, G. Cui, H. Feng, L. Chen, H. Wang, B. Wang, X. Zhang, L. Zheng, S. Hong and M. Wei, Platinum-copper single atom alloy catalysts with high performance towards glycerol hydrogenolysis, *Nat. Commun.*, 2019, **10**, 5812.

39 G. Sun, Z. J. Zhao, R. Mu, S. Zha, L. Li, S. Chen, K. Zang, J. Luo, Z. Li, S. C. Purdy, A. J. Kropf, J. T. Miller, L. Zeng and J. Gong, Breaking the scaling relationship via thermally stable Pt/Cu single atom alloys for catalytic dehydrogenation, *Nat. Commun.*, 2018, **9**(1), 4454.

40 I. S. Mashkovsky, P. V. Markov, A. V. Rassolov, E. D. Patil and A. Y. Stakheev, Progress in single-atom methodology in modern catalysis, *Russ. Chem. Rev.*, 2023, **92**(8), 5087.

41 G. X. Pei, X. Y. Liu, A. Wang, A. F. Lee, M. A. Isaacs, L. Li, X. Pan, X. Yang, X. Wang, Z. Tai, K. Wilson and T. Zhang, Ag Alloyed Pd Single-Atom Catalysts for Efficient Selective Hydrogenation of Acetylene to Ethylene in Excess Ethylene, *ACS Catal.*, 2015, **5**(6), 3717–3725.

42 G. Pei, X. Liu, M. Chai, A. Wang and T. Zhang, Isolation of Pd atoms by Cu for semi-hydrogenation of acetylene: Effects of Cu loading, *Chin. J. Catal.*, 2017, **38**(9), 1540–1548.

43 J. Liu, J. Shan, F. R. Lucci, S. Cao, E. C. H. Sykes and M. Flytzani-Stephanopoulos, Palladium-gold single atom alloy catalysts for liquid phase selective hydrogenation of 1-hexyne, *Catal. Sci. Technol.*, 2017, **7**(19), 4276–4284.

44 M. J. Islam, M. G. Mesa, A. Osatiashtiani, J. C. Manayil, M. A. Isaacs, M. J. Taylor, S. Tsatsos and G. Kyriakou, PdCu single atom alloys supported on alumina for the selective hydrogenation of furfural, *Appl. Catal., B*, 2021, **299**, 120652.

45 T. Zhang, P. Zheng, J. Gao, Z. Han, F. Gu, W. Xu, L. Li, T. Zhu, Z. Zhong, G. Xu and F. Su, Single-Atom Ru Alloyed with Ni Nanoparticles Boosts CO2 Methanation, *Small*, 2023, e2308193.

46 M. B. Boucher, B. Zugic, G. Cladaras, J. Kammert, M. D. Marcinkowski, T. J. Lawton, E. C. H. Sykes and M. Flytzani-Stephanopoulos, Single atom alloy surface analogs in $Pd_{0.18}Cu_{15}$ nanoparticles for selective hydrogenation reactions, *Phys. Chem. Chem. Phys.*, 2013, **15**(29), 12187–12196.

47 X. Cao, A. Mirjalili, J. Wheeler, W. Xie and B. W. L. Jang, Investigation of the preparation methodologies of Pd-Cu single atom alloy catalysts for selective hydrogenation of acetylene, *Front. Chem. Sci. Eng.*, 2015, **9**(4), 442–449.

48 Z. Sun, J. Masa, W. Xia, D. König, A. Ludwig, Z.-A. Li, M. Farle, W. Schuhmann and M. Muhler, Rapid and Surfactant-Free Synthesis of Bimetallic Pt–Cu Nanoparticles Simply via Ultrasound-Assisted Redox Replacement, *ACS Catal.*, 2012, **2**(8), 1647–1653.

49 Y. Zhao, J. Liu, C. Liu, F. Wang and Y. Song, Amorphous CuPt Alloy Nanotubes Induced by Na2S2O3 as Efficient Catalysts for the Methanol Oxidation Reaction, *ACS Catal.*, 2016, **6**(7), 4127–4134.

50 M. Mohl, D. Dobo, A. Kukovecz, Z. Konya, K. Kordas, J. Wei, R. Vajtai and P. M. Ajayan, Formation of CuPd and CuPt Bimetallic Nanotubes by Galvanic Replacement Reaction, *J. Phys. Chem. C*, 2011, **115**(19), 9403–9409.

51 M. J. Islam, M. Granollers Mesa, A. Osatiashtiani, M. J. Taylor, M. A. Isaacs and G. Kyriakou, The Hydrogenation of Crotonaldehyde on PdCu Single Atom Alloy Catalysts, *Nanomaterials*, 2023, **13**(8), 1434.

52 F. R. Lucci, J. Liu, M. D. Marcinkowski, M. Yang, L. F. Allard, M. Flytzani-Stephanopoulos and E. C. Sykes, Selective hydrogenation of 1,3-butadiene on platinum-copper alloys at the single-atom limit, *Nat. Commun.*, 2015, **6**, 8550.

53 F. R. Lucci, J. Liu, M. D. Marcinkowski, M. Yang, L. F. Allard, M. Flytzani-Stephanopoulos and E. C. H. Sykes, Selective hydrogenation of 1,3-butadiene on platinum-copper alloys at the single-atom limit, *Nat. Commun.*, 2015, **6**, 8550.

54 J. Shan, J. Liu, M. Li, S. Lustig, S. Lee and M. Flytzani-Stephanopoulos, NiCu single atom alloys catalyze the C-H bond activation in the selective non- oxidative ethanol dehydrogenation reaction, *Appl. Catal., B*, 2018, **226**, 534–543.

55 H. Zhang, K. Kawashima, M. Okumura and N. Toshima, Colloidal Au single-atom catalysts embedded on Pd nanoclusters, *J. Mater. Chem. A*, 2014, **2**(33), 13498–13508.

56 K. Ji, M. Xu, S.-M. Xu, Y. Wang, R. Ge, X. Hu, X. Sun and H. Duan, Electrocatalytic Hydrogenation of 5-Hydroxymethylfurfural Promoted by a Ru1Cu Single-Atom Alloy Catalyst, *Angew. Chem., Int. Ed.*, 2022, e202209849.

57 M. T. Darby, M. Stamatakis, A. Michaelides and E. C. H. Sykes, Lonely Atoms with Special Gifts: Breaking Linear Scaling Relationships in Heterogeneous Catalysis with Single-Atom Alloys, *J. Phys. Chem. Lett.*, 2018, **9**(18), 5636–5646.

58 Z.-T. Wang, R. A. Hoyt, M. El-Soda, R. J. Madix, E. Kaxiras and E. C. H. Sykes, Dry Dehydrogenation of Ethanol on Pt–Cu Single Atom Alloys, *Top. Catal.*, 2017, **61**(5–6), 328–335.

59 D. A. Patel, R. T. Hannagan, P. L. Kress, A. C. Schilling, V. Çınar and E. C. H. Sykes, Atomic-Scale Surface Structure and CO Tolerance of NiCu Single-Atom Alloys, *J. Phys. Chem. C*, 2019, **123**(46), 28142–28147.

60 M. D. Marcinkowski, M. T. Darby, J. Liu, J. M. Wimble, F. R. Lucci, S. Lee, A. Michaelides, M. Flytzani-Stephanopoulos, M. Stamatakis and E. C. H. Sykes, Pt/Cu single-atom alloys as coke-resistant catalysts for efficient C-H activation, *Nat. Chem.*, 2018, **10**(3), 325–332.

61 F. R. Lucci, M. D. Marcinkowski, T. J. Lawton and E. C. H. Sykes, H2 Activation and Spillover on Catalytically

Relevant Pt–Cu Single Atom Alloys, *J. Phys. Chem. C*, 2015, **119**(43), 24351–24357.

62 H. Liu, P. Jin, Y. M. Xue, C. Dong, X. Li, C. C. Tang and X. W. Du, Photochemical Synthesis of Ultrafine Cubic Boron Nitride Nanoparticles under Ambient Conditions, *Angew. Chem., Int. Ed.*, 2015, **54**(24), 7051–7054.

63 C. H. Chen, D. Wu, Z. Li, R. Zhang, C. G. Kuai, X.-R. Zhao, C. K. Dong, S. Z. Qiao, H. Liu and X.-W. Du, Ruthenium-Based Single-Atom Alloy with High Electrocatalytic Activity for Hydrogen Evolution, *Adv. Energy Mater.*, 2019, **9**(20), 1803913.

64 X. Li, P. Shen, Y. Luo, Y. Li, Y. Guo, H. Zhang and K. Chu, PdFe Single-Atom Alloy Metallene for N2 Electroreduction, *Angew. Chem., Int. Ed.*, 2022, **61**, e202205923.

65 C. Yang, Z. Miao, F. Zhang, L. Li, Y. Liu, A. Wang and T. Zhang, The Hydrogenation of Crotonaldehyde on PdCu Single Atom Alloy Catalysts, *Nanomaterials*, 2023, **13**(8), 1434.

66 C. Du, J. P. Mills, A. G. Yohannes, W. Wei, L. Wang, S. Lu, J.-X. Lian, M. Wang, T. Guo, X. Wang, H. Zhou, C.-J. Sun, J. Z. Wen, B. Kendall, M. Couillard, H. Guo, Z. Tan, S. Siahrostami and Y. A. Wu, Cascade electrocatalysis via AgCu single-atom alloy and Ag nanoparticles in CO_2 electroreduction toward multicarbon products, *Nat. Commun.*, 2023, **14**(1), 6142.

67 J. Li, X. Liang and C. Zhao, Constructing poison-resistant Au-Pd single-atom alloy electrocatalyst on Pd nanocrystals for formic acid electrooxidation, *Int. J. Electrochem. Sci.*, 2023, **18**(6), 100173.

68 H. Zhang and N. Toshima, Crown Jewel-Structured Au/Pd Nanoclusters as Novel Catalysts for Aerobic Glucose Oxidation, *J. Nanosci. Nanotechnol.*, 2013, **13**(8), 5405–5412.

69 B. Geng, L. Zhang, F. Wang, X. Wang, S. Song and H. Zhang, Recent Progress of Single-Atom Alloys in Heterogeneous Catalytic Reactions, *Eur. J. Inorg. Chem.*, 2023, **26**(14), e202300052.

70 X. Xu, Q. Wang, L. Xie, Y. Liu, D. Li, J. Feng and X. Duan, Thermal effect optimization endows a selective and stable PdCu single atom alloy catalyst for acetylene hydrogenation, *AIChE J.*, 2023, **69**(6), e18042.

71 J. Zhang, L. Wang, Y. Shao, Y. Wang, B. C. Gates and F.-S. Xiao, A Pd@Zeolite Catalyst for Nitroarene Hydrogenation with High Product Selectivity by Sterically Controlled Adsorption in the Zeolite Micropores, *Angew. Chem., Int. Ed.*, 2017, **56**(33), 9747–9751.

72 X. Huang, Y. Xia, Y. Cao, X. Zheng, H. Pan, J. Zhu, C. Ma, H. Wang, J. Li, R. You, S. Wei, W. Huang and J. Lu, Enhancing both selectivity and coking-resistance of a single-atom Pd_1/C_3N_4 catalyst for acetylene hydrogenation, *Nano Res.*, 2017, **10**(4), 1302–1312.

73 S. Zhang, C.-R. Chang, Z.-Q. Huang, J. Li, Z. Wu, Y. Ma, Z. Zhang, Y. Wang and Y. Qu, High Catalytic Activity and Chemoselectivity of Sub-nanometric Pd Clusters on Porous Nanorods of CeO_2 for Hydrogenation of Nitroarenes, *J. Am. Chem. Soc.*, 2016, **138**(8), 2629–2637.

74 G. X. Pei, X. Y. Liu, X. Yang, L. Zhang, A. Wang, L. Li, H. Wang, X. Wang and T. Zhang, Performance of Cu-Alloyed Pd Single-Atom Catalyst for Semihydrogenation of Acetylene under Simulated Front-End Conditions, *ACS Catal.*, 2017, **7**(2), 1491–1500.

75 C. M. Kruppe, J. D. Krooswyk and M. Trenary, Selective Hydrogenation of Acetylene to Ethylene in the Presence of a Carbonaceous Surface Layer on a Pd/Cu(111) Single-Atom Alloy, *ACS Catal.*, 2017, **7**(12), 8042–8049.

76 S. Shao, Y. Yang, K. Sun, S. Yang, A. Li, F. Yang, X. Luo, S. Hao and Y. Ke, Electron-Rich Ruthenium Single-Atom Alloy for Aqueous Levulinic Acid Hydrogenation, *ACS Catal.*, 2021, **11**(19), 12146–12158.

77 X. Dai, Z. Chen, T. Yao, L. Zheng, Y. Lin, W. Liu, H. Ju, J. Zhu, X. Hong, S. Wei, Y. Wu and Y. Li, Single Ni sites distributed on N-doped carbon for selective hydrogenation of acetylene, *Chem. Commun.*, 2017, **53**(84), 11568–11571.

78 X. Cao, Q. Fu and Y. Luo, Catalytic activity of Pd-doped Cu nanoparticles for hydrogenation as a single-atom-alloy catalyst, *Phys. Chem. Chem. Phys.*, 2014, **16**(18), 8367–8375.

79 H. Zhu, D. H. Anjum, Q. Wang, E. Abou-Hamad, L. Emsley, H. Dong, P. Laveille, L. Li, A. K. Samal and J.-M. Basset, Sn surface-enriched Pt–Sn bimetallic nanoparticles as a selective and stable catalyst for propane dehydrogenation, *J. Catal.*, 2014, **320**, 52–62.

80 J. J. H. B. Sattler, J. Ruiz-Martinez, E. Santillan-Jimenez and B. M. Weckhuysen, Catalytic Dehydrogenation of Light Alkanes on Metals and Metal Oxides, *Chem. Rev.*, 2014, **114**(20), 10613–10653.

81 R. J. J. Bunting, F. Wodaczek, T. Torabi and B. Cheng, Reactivity of Single-Atom Alloy Nanoparticles: Modeling the Dehydrogenation of Propane, *J. Am. Chem. Soc.*, 2023, **145**(27), 14894–14902.

82 P. Sun, G. Siddiqi, M. Chi and A. T. Bell, Synthesis and characterization of a new catalyst Pt/Mg(Ga)(Al)O for alkane dehydrogenation, *J. Catal.*, 2010, **274**(2), 192–199.

83 X. Chen, M. Peng, X. Cai, Y. Chen, Z. Jia, Y. Deng, B. Mei, Z. Jiang, D. Xiao, X. Wen, N. Wang, H. Liu and D. Ma, Regulating coordination number in atomically dispersed Pt species on defect-rich graphene for n-butane dehydrogenation reaction, *Nat. Commun.*, 2021, **12**(1), 2664.

84 M. D. Marcinkowski, J. Liu, C. J. Murphy, M. L. Liriano, N. A. Wasio, F. R. Lucci, M. Flytzani-Stephanopoulos and E. C. H. Sykes, Selective Formic Acid Dehydrogenation on Pt-Cu Single-Atom Alloys, *ACS Catal.*, 2017, **7**(1), 413–420.

85 Y. Zhang, B. Wang, M. Fan, D. Li and R. Zhang, Ethane dehydrogenation over the single-atom alloy catalysts: Screening out the excellent catalyst with the dual descriptors, *Fuel*, 2021, **306**, 121641.

86 J. Shan, F. R. Lucci, J. Liu, M. El-Soda, M. D. Marcinkowski, L. F. Allard, E. C. H. Sykes and M. Flytzani-Stephanopoulos, Water co-catalyzed selective dehydrogenation of methanol to formaldehyde and hydrogen, *Surf. Sci.*, 2016, **650**, 121–129.

87 Z.-T. Wang, R. A. Hoyt, M. El-Soda, R. J. Madix, E. Kaxiras and E. C. H. Sykes, Dry Dehydrogenation of Ethanol on Pt-Cu Single Atom Alloys, *Top. Catal.*, 2018, **61**(5–6), 328–335.

88 X. Bai, Z. Zhao and G. Lu, Breaking the Scaling Relationship on Single-Atom Embedded MBene for Selective CO_2

Electroreduction, *J. Phys. Chem. Lett.*, 2023, **14**(22), 5172–5180.

89 C. Qiao and G. Fu, Activation of single atom alloys towards alkyl C-H bond: A theoretical study, *Chin. J. Chem. Phys.*, 2023, **36**(4), 427–433.

90 S. Sun, G. Sun, C. Pei, Z.-J. Zhao and J. Gong, Origin of Performances of Pt/Cu Single-Atom Alloy Catalysts for Propane Dehydrogenation, *J. Phys. Chem. C*, 2021, **125**(34), 18708–18716.

91 X. Liu, X. Wang, S. Zhen, G. Sun, C. Pei, Z.-J. Zhao and J. Gong, Support stabilized PtCu single-atom alloys for propane dehydrogenation, *Chem. Sci.*, 2022, **13**(33), 9537–9543.

92 A. S. Hashmi and G. J. Hutchings, Gold catalysis, *Angew. Chem., Int. Ed.*, 2006, **45**(47), 7896–7936.

93 B. Nan, L. Li, Y. Li, L. Guo, M. Du, Z. Liu, X. Tao, C. Tian, Z. Liang, Y. Zhang, C. Ma, L. Shen, R. Si and L. Li, Hydrogen-controlled structural reconstruction of palladium-bismuth oxide cluster to single atom alloy for low-temperature CO oxidation, *Appl. Catal., B*, 2023, **334**, 122818.

94 X. Gu, Z. H. Lu, H. L. Jiang, T. Akita and Q. Xu, Synergistic catalysis of metal-organic framework-immobilized Au-Pd nanoparticles in dehydrogenation of formic acid for chemical hydrogen storage, *J. Am. Chem. Soc.*, 2011, **133**(31), 11822–11825.

95 C. J. Wrasman, A. Boubnov, A. R. Riscoe, A. S. Hoffman, S. R. Bare and M. Cargnello, Synthesis of Colloidal Pd/Au Dilute Alloy Nanocrystals and Their Potential for Selective Catalytic Oxidations, *J. Am. Chem. Soc.*, 2018, **140**(40), 12930–12939.

96 H. Zhang, T. Watanabe, M. Okumura, M. Haruta and N. Toshima, Catalytically highly active top gold atom on palladium nanocluster, *Nat. Mater.*, 2012, **11**, 49–52.

97 L. Zhou, Y.-Q. Su and T.-L. Hu, Theoretical insights into the selective oxidation of methane to methanol on single-atom alloy catalysts, *Sci. China Mater.*, 2023, **66**(8), 3189–3199.

98 S. Luo, L. Zhang, Y. Liao, L. Li, Q. Yang, X. Wu, X. Wu, D. He, C. He, W. Chen, Q. Wu, M. Li, E. J. M. Hensen and Z. Quan, A Tensile-Strained Pt-Rh Single-Atom Alloy Remarkably Boosts Ethanol Oxidation, *Adv. Mater.*, 2021, **33**(17), 2008508.

99 Y. Meng, C. Ding, X. Gao, L. Ma, K. Zhang, J. Wang and Z. Li, Adsorption of Pd on the Cu(111) surface and its catalysis of methane partial oxidation: A density functional theory study, *Appl. Surf. Sci.*, 2020, **513**, 145724.

100 Y. Zhang, X.-R. Shi, C. Sun, S. Huang, Z. Duan, P. Ma and J. Wang, CO oxidation on Ni-based single-atom alloys surfaces, *Mol. Catal.*, 2020, **495**, 111154.

101 J. Shan, G. Giannakakis, J. Liu, S. Cao, M. Ouyang, M. Li, S. Lee and M. Flytzani-Stephanopoulos, PdCu Single Atom Alloys for the Selective Oxidation of Methanol to Methyl Formate at Low Temperatures, *Top. Catal.*, 2020, **63**(7–8), 618–627.

102 H. Li, W. Chai and G. Henkelman, Selectivity for ethanol partial oxidation: the unique chemistry of single-atom alloy catalysts on Au, Ag, and Cu(111), *J. Mater. Chem. A*, 2019, **7**(41), 23868–23877.

103 S. Baskaran, C.-Q. Xu, Y.-G. Wang, I. L. Garzon and J. Li, Catalytic mechanism and bonding analyses of Au-Pd single atom alloy (SAA): CO oxidation reaction, *Sci. China Mater.*, 2020, **63**(6), 993–1002.

104 A. R. Poerwoprajitno, L. Gloag, J. Watt, S. Cheong, X. Tan, H. Lei, H. A. Tahini, A. Henson, B. Subhash, N. M. Bedford, B. K. Miller, P. B. O'Mara, T. M. Benedetti, D. L. Huber, W. Zhang, S. C. Smith, J. J. Gooding, W. Schuhmann and R. D. Tilley, A single-Pt-atom-on-Ru-nanoparticle electrocatalyst for CO-resilient methanol oxidation, *Nat. Catal.*, 2022, **5**(3), 231–237.

105 H. Wang, L. Jiao, L. Zheng, Q. Fang, Y. Qin, X. Luo, X. Wei, L. Hu, W. Gu, J. Wen and C. Zhu, PdBi Single-Atom Alloy Aerogels for Efficient Ethanol Oxidation, *Adv. Funct. Mater.*, 2021, **31**(38), 2103465.

106 J. Liu, F. R. Lucci, M. Yang, S. Lee, M. D. Marcinkowski, A. J. Therrien, C. T. Williams, E. C. H. Sykes and M. Flytzani-Stephanopoulos, Tackling CO Poisoning with Single-Atom Alloy Catalysts, *J. Am. Chem. Soc.*, 2016, **138**(20), 6396–6399.

107 L. Hui, Y. Xue, C. Xing, Y. Liu, Y. Du, Y. Fang, H. Yu, C. Zhang, F. He and Y. Li, Atomic alloys of nickel-platinum on carbon network for methanol oxidation, *Nano Energy*, 2022, **95**, 106984.

108 Y. Meng, C. Ding, X. Gao, l. Ma, K. Zhang, J. Wang and Z. Li, Adsorption of Pd on the Cu(1 1 1) surface and its catalysis of methane partial oxidation: A density functional theory study, *Appl. Surf. Sci.*, 2020, **513**, 145724.

109 Q. Wang, J. Gong, H. Zhang, Q.-Y. Fan, L. Xue, J. Wu, J. Li, Y. Wang, Z. Liu, R. Gao and S. Zeng, Co-promotion of two-type active sites: PtCux single-atom alloy and copper-ceria interface for preferential oxidation of CO, *Appl. Catal., B*, 2022, **306**, 121117.

110 H. Wang, Q. Luo, W. Liu, Y. Lin, Q. Guan, X. Zheng, H. Pan, J. Zhu, Z. Sun, S. Wei, J. Yang and J. Lu, Quasi Pd1Ni single-atom surface alloy catalyst enables hydrogenation of nitriles to secondary amines, *Nat. Commun.*, 2019, **10**(1), 4998.

111 T. Gan, Y. Liu, Q. He, H. Zhang, X. He and H. Ji, Facile Synthesis of Kilogram-Scale Co-Alloyed Pt Single-Atom Catalysts via Ball Milling for Hydrodeoxygenation of 5-Hydroxymethylfurfural, *ACS Sustainable Chem. Eng.*, 2020, **8**(23), 8692–8699.

112 J.-q. Bai, M. Tamura, A. Nakayama, Y. Nakagawa and K. Tomishige, Comprehensive Study on Ni- or Ir-Based Alloy Catalysts in the Hydrogenation of Olefins and Mechanistic Insight, *ACS Catal.*, 2021, **11**(6), 3293–3309.

113 Y. Xing, L. Kang, J. Ma, Q. Jiang, Y. Su, S. Zhang, X. Xu, L. Li, A. Wang, Z. P. Liu, S. Ma, X. Y. Liu and T. Zhang, Sn1Pt single-atom alloy evolved stable PtSn/nano-Al_2O_3 catalyst for propane dehydrogenation, *Chin. J. Catal.*, 2023, **48**, 164–174.

114 B. Nan, L. Li, Y. Li, L. Guo, M. Du, Z. Liu, X. Tao, C. Tian, Z. Liang, Y. Zhang, C. Ma, L. Shen, R. Si and L. Li, Hydrogen-controlled structural reconstruction of palladium-bismuth oxide cluster to single atom alloy for low-temperature CO oxidation, *Appl. Catal., B*, 2023, **334**, 122818.